Characterization of Peptides Corresponding to the Seven Transmembrane Domains of Human Adenosine A_2a Receptor†

Tzvetana Lazarova,‡ Krista A. Brewin,‡ Kristin Stoeber,§ and Clifford R. Robinson*,‡,§,||

Department of Chemistry and Biochemistry and Department of Chemical Engineering, Delaware Biotechnology Institute, University of Delaware, Newark, Delaware 19711

Received April 20, 2004; Revised Manuscript Received August 3, 2004

ABSTRACT: Human adenosine A_2a receptor is a member of the G-protein-coupled receptor (GPCR) superfamily of seven-helix transmembrane (TM) proteins. To test general models for membrane-protein folding and to identify specific features of folding and assembly for this representative member of an important and poorly understood class of proteins, we synthesized peptides corresponding to its seven TM domains. We assessed the ability of the peptides to insert into micelles and vesicles and measured secondary structure for each peptide in aqueous and membrane-mimetic environments. CD spectra indicate that each of the seven TM peptides form thermally stable, independent α-helical structures in both micelles and vesicles. The helical content of the peptides depends on the nature of the membrane-mimetic environment. Four of the peptides (TM3, TM4, TM5, and TM7) exhibit very high-helical structure, near the predicted maximum for their TM segments. The TM1 peptide also adopts relatively high α-helical structures. In contrast, two of peptides, TM2 and TM6, display low α helicity. Similarly, the ability of the peptides to insert into membrane-mimetic environments, assayed by intrinsic tryptophan fluorescence and fluorescence quenching, varied markedly. Most peptides exhibit higher α helicity in anionic sodium dodecyl sulfate than in neutral dodecyl-*β*-D-maltoside micelles, and TM2 was disordered in zwiterionic DMPC but was α-helical in negatively charged DMPC/DMPG vesicles. These findings strongly suggest that electrostatic interactions between lipids and peptides control the insertion of the peptides and may be involved in membrane-protein-folding events. The measured helical content of these TM domains does not correlate with the predicted helicity based on amino acid sequence, pointing out that, while hydrophobic interactions can be a major determinant for folding of TM peptides, other factors, such as electrostatic interactions or helix−helix interactions, may play significant roles for specific TM domains. Our results represent a comprehensive analysis of helical propensities for a human GPCR and support models for membrane-protein folding in which interactions between TM domains are required for proper insertion and folding of some TM helix domains. The tendency of some peptides to self-associate, especially in aqueous environments, underscores the need to prevent improper interactions during folding and refolding of membrane proteins in vivo and in vitro.

Adenosine A_2a receptor belongs to one of the largest family of membrane proteins, the G-protein-coupled receptors (GPCRs).[1] The GPCRs are cell-surface receptors that mediate signal transduction across the plasma membrane. They are involved in a wide variety of physiological processes and are implicated in numerous human diseases (*1*−*3*). Nearly two-thirds of marketed drugs target GPCRs, and it is estimated that as much as 70% of current drug discovery efforts are aimed at GPCRs (*2*). Despite their importance, the molecular mechanisms of GPCR ligand discrimination, activation, and signaling remain unclear (*4*).

Production of large amounts of GPCRs is a major obstacle, and severely hinders crystallization efforts and structural analysis (*5*). Of the thousands of GPCRs, the structure of only one, bovine rhodopsin, has been determined at high resolution (*6*). While the mechanism of GPCR activation is thought to be general, GPCR sequences vary widely, and it is not known whether all GPCRs have similar structures (*6*−*8*). Differences in helix orientation, helix−helix interactions, and topology may exist. Therefore, a clear need exists for detailed structural studies to improve our understanding of the structure and function of the GPCR family. The difficulties associated with GPCR structure determination and biophysical analyses arise, in part, from our limited understanding of membrane-protein folding, assembly, and stability.

In the two-stage model for integral-membrane-protein folding, transmembrane domains (TMDs) form independent stable helices in the membrane, which associate to form the active native structure (*9*). The two-stage model was first

† This research was supported by NIH 1-P20-RR017716-01.

* To whom correspondence should be addressed: Department of Chemistry and Biochemistry, Delaware Biotechnology Institute, 15 Innovation Way, University of Delaware, Newark, DE 19711. E-mail: robinson@dbi.udel.edu. Telephone: 302-831-4942. Fax: 302-831-3447.

‡ Department of Chemistry and Biochemistry.

§ Department of Chemical Engineering.

|| Delaware Biotechnology Institute.

[1] Abbreviations: GPCR, G-protein-coupled receptor; TMD, transmembrane domain; cmc, critical micelle concentration; CD, circular dichroism; SDS, sodium dodecyl sulfate; D*β*M, *n*-dodecyl-*β*-D-maltoside; T_m, temperature of phase transition; AFM, atomic force microscopy; BR, bacteriorhodopsin.

10.1021/bi0492051 CCC: $27.50
Published on Web 09/16/2004

tested experimentally using peptides representing the seven TMDs of bacteriorhodopsin (BR) (*10*). Five of the peptides indeed form stable independent helical structures in the lipid bilayer, but the others showed low degrees of membrane partitioning and form non-native secondary structures. Analogous studies of the yeast Ste2 receptor showed that five of the seven TMDs form stable helices in micelles or vesicles, while the other two formed β sheets and/or aggregates (*11*). In both cases, it is envisioned that the folding of these helices in the context of the full-length protein might occur by more complex processes and involve some external constraints or interactions with other helices (*12*, *13*). In the past few years, in vivo and in vitro studies of membrane proteins and helical-membrane peptides have shed more light on the folding process and mechanisms (*14*−*25*).

Major outstanding questions include how TMD stability and helical propensity relate to membrane insertion, and whether TMDs have equivalent properties, as suggested by framework models for membrane-protein folding, or whether cofolding of TMDs might be generally required in assembly of large, multihelix membrane proteins. The stability of single TM helices inserted in the bilayer and the evident applicability of the two-stage model provide a framework in which the forces involved in TM helix stability can be studied separately from those involved in TM helix association. One such approach is to study peptides corresponding to individual TMDs (*10*, *26*−*28*). Although long-range interactions are disabled in such studies, the ability of BR and rhodopsin fragments to assemble into active forms verifies the relevance of this approach (*29*, *30*).

We are studying stability and assembly of the human adenosine A_2a receptor, as a representative example of the human GPCRs. The adenosine family of receptors has been linked to cardioprotective and antihypertensive effects during periods of stress such as hypoxia or ischemia (*31*). A_2a activates adenylate cyclase through coupling to G_s, which results in multiple actions including vasodilation. Adenosine receptors are important targets in the search for the molecular origins of cardiovascular disease, and numerous biomedical, clinical, and drug discovery efforts are aimed at these receptors (*31*, *32*).

We sought to test current models for membrane-protein folding by evaluating helicity and insertion of the TMDs of the human adenosine A_2a receptor, as a complement to our ongoing studies of the full-length receptor. In this study, we designed model peptides corresponding to the seven TMDs of A_2a and studied their folding capacities and stability in membrane-mimetic environments: detergent micelles and lipid vesicles. We used fluorescence spectroscopy to monitor the binding of peptides to vesicles and micelles and circular dichroism (CD) spectroscopy to examine their 2° structures. We find that the helicity and insertion propensities of these peptides vary significantly, suggesting that assembly of the A_2a receptor may occur from incompletely formed helices, that interhelical or long-range interactions may precede or assist the membrane-insertion process for some TMDs, and that long-range interactions may be required to induce helicity in several of the TMDs of this GPCRs.

MATERIALS AND METHODS

Peptide Synthesis. Peptides were synthesized and purchased from Ana Spec Inc. All of the seven peptides were purified to >95% purity as judged by HPLC. The identity of the purified peptides was confirmed by mass spectrometry. Peptides were stored at −20 °C as solid powders.

Peptide Concentration. The peptide concentration was determined using two different approaches: by amino acid analysis (performed at Purdue University Core Facility PSAL) or spectrophotometricaly by measuring UV absorbance spectra of the peptides in 6 M Gdn/HCl solutions at 280 nm, using appropriate extinction coefficients for the aromatic Trp and Tyr residues (*33*). Prior to measurements, peptide stock solutions (at about 2 mg/mL) were prepared in water or in water/tetrafluoroethylene (TFE) solutions (for TM peptides 1, 2, and 4), as described previously for highly hydrophobic peptides (*10*).

Preparation of Vesicles and Micelles. DMPC and DMPG lipids were purchased from Avanti Polar Lipids. The lipid films were prepared by dissolving about 10 mg of lipid in chloroform/methanol (2:1) and drying under a steam of N_2. The residual organic solvents were removed by keeping the lipid film under high vacuum for several hours. The dry lipid film was hydrated in 10 mM Tris at pH 7 for at least 30 min at a temperature above the temperature of the phase transition (T_m) of DMPC, with periodic vortexing. The resulting multilamellar vesicles were freeze-thawed in liquid nitrogen for seven cycles and were extruded through two stacked polycarbonate membranes (with a pore size of 100 nm) using a Mini Extruder (Lipofast, Avestin, Ottawa, Canada) to obtain large unilamellar vesicles (LUV). Liposomes were used immediately following their preparation, or stored briefly at temperatures above their T_m. DMPC/DMPG films were prepared by dissolving appropriate amounts of each of the lipid components in methanol and mixing these solutions to give the desired molar ratio. The solvent was removed by drying under a nitrogen stream, and the LUV was prepared as described above.

Three different detergents were used to prepare micelles: sodium dodecyl sulfate (SDS), dodecyl-β-D-maltoside (DβM), and Triton X-100. The micelles were prepared in 10 mM Tris-HCl buffer at pH 7. The concentration of each detergent was always well above the critical micelle concentration (cmc) (*34*).

Fluorescence Measurements. Fluorescence measurements were performed on an ISS PC-1 spectrofluorimeter, operating in photon-counting mode, using 10 × 10- or 2 × 10-mm quartz cuvettes. The excitation wavelength was 295 or 280 nm, and the emission was scanned from 300 to 500 nm. To minimize light-scattering effects, all scans were performed with polarizers in place, with the emission polarizer oriented at 0° and the excitation polarizer at 90° (*35*). In all experiments, appropriate reference spectra, with either the buffer alone or the buffer containing micelles or liposomes, were subtracted from the sample spectra. The peptide concentration in all fluorescence measurements was maintained constant at about 1−3 μM. The experiments with DMPC vesicles were performed at 35 °C, which is well above the T_m of the lipid (23 °C). In the liposome-binding experiments, the peptide (at about 1−2 μM) was titrated by adding small aliquots (1−8 μL) of the liposome stock solution (5 mM). For fluorescence-quenching experiments, small aliquots of 4 M acrylamide stock solution were added to the peptides in the absence or presence of micelles and the fluorescence emission spectra were recorded. To reduce

Table 1: Sequences of the Seven Peptides Corresponding to the TMDs of the Adenosine A_2a Receptor

amino acid sequences[a]	name	R^b	H (KD)[c]
KKK **VYITVELAIAVLAILGNVLVCWA** *KKKK*	TM1	30 (23)	2.14
KKK **FVVSLAAADIAVGVLAIPWAITI** *KKKK*	TM2	30 (23)	2.09
KKK **LFIAAFVLVLTQSSIFSLLAIAI** ***DRY****KKK*	TM3	32 (23)	2.4
*KKK****R*****AKGIIAICWVLSFAIGLTPMLGW** *KKKK*	TM4	31 (23)	1.51
*KKK***MNYMVWFNFFACVLVPLLLMLGVYL** ***R****KKK*	TM5	32 (25)	1.75
*KKK***LAIIVGLFALAWLPLHIINAFTFF*****CPD*** *KK*	TM6	32 (24)	2.05
KKK **LWLMYLAIVLSHTNSVVNPFIYAY*****RIRE****K*	TM7	32 (24)	1.09

[a] Residues predicted to be part of the TMDs (http://www.gpcr.org/7tm/) are indicated in bold, and those predicted to be in loops are in bold and italics. The residues that differ from the native A_2a sequence are underlined: in the TM2 and TM5, F and Y, respectively, are substituted for W, to monitor the peptide binding to the membrane; in TM3 and TM6 one and two C, respectively, are replaced by A. The Lys added at the N and C termini are indicated in italics. [b] The first number represents the total number of residues in the peptide; the second number in parentheses represents the number of residues in the putative TM domain. [c] Average hydrophobicity of the peptides as calculated using the Kyte−Doolittle scale (*61*).

the absorbance of acrylamide at 280 nm, the samples were excited at 295 nm. The data were analyzed according to the Stern−Volmer equation

$$F_0/F = 1 + K_{SV}[Q]$$

where F_0 and F are the fluorescence intensities in the absence and presence of the quencher and K_{SV} is the Stern−Volmer quenching constant, which is a measure of the accessibility of Trp residues to acrylamide (*36*).

CD Measurements. Far-UV CD spectra of the peptides were recorded on an Aviv model 202 spectrometer, equipped with a Peltier thermal-controlled cuvette holder. To ensure that the CD spectra were observed from peptides in solution, several steps were taken. Although differential light scattering and absorption flattering are typically only observed for large proteins (e.g., BR), rather than peptides in micelles or vesicles, spectra conditions were chosen to minimize those effects (*37*−*39*). The spectra were recorded using a 0.1-cm path-length quartz cuvette, from 260 to 190 nm, at a 1-nm step resolution and an integration time of 3 s. All spectra are averages from at least four individual spectra. In each case, appropriate reference spectra of the buffer, micelles, or liposomes were recorded under identical conditions and subtracted from the CD spectra acquired for the peptides. Dynode voltage was recorded, and the spectra were recorded only in the linear range of the dynode values. In thermal stability experiments, the samples were incubated for 10 min at each temperature to allow equilibration prior to recording spectra. Peptide concentrations used in CD experiments were in the range of 10−30 μM. Peptide/lipid molar ratios were 1:100 for measurements in vesicles.

CD intensities are expressed in mean residue molar ellipticity $[\theta]$, calculated from the equation

$$[\theta] = \theta_{obs}/10lcn \quad (\text{in degrees cm}^2\ \text{dmol}^{-1})$$

where θ_{obs} is the observed ellipticity in millidegrees, l is the optical path length in centimeters, c is the final concentration of the peptides in molars, and n is number of the amino acid residues. The percentage helicity was calculated according to the method of Chen et al., using an empirical equation for helix length dependence, assuming that the residue ellipticity at 222 nm is exclusively due to α helix

$$\text{percentage of } \alpha \text{ helix} = [\theta]_{222}/[\theta]_{222}^{max}(1 - (k/n)) \quad (\text{in degrees cm}^2\ \text{dmol}^{-1})$$

where $[\theta]_{222}$ is the observed mean residue ellipticity at 222 nm, $[\theta]_{222}^{max}$ is theoretical mean residue ellipticity for a helix of infinite length (−39 500 at 222 nm), n is number of the residues, and k is a wavelength-dependent constant (2.57 for 222 nm) (*40*, *41*). Although this is a relatively old method and fairly simple compared to more modern techniques, recent studies have shown that this method remains the most reliable for calculating the helicity of TM peptides (*11*, *42*)

Peptide Design. Table 1 shows the amino sequences of the peptides used in this study. The peptides were designed to correspond to the seven TMDs of the human adenosine A_2a receptor. Our first attempt to synthesize and purify the model peptides, using the exact sequence of the predicted TMDs and intra- and extracellular loops, was not successful. Because of their extremely high hydrophobicity, the synthesized peptides absorbed irreversibly to the HPLC columns, and we could not achieve sufficient purification. To overcome this difficulty, a few small modifications were made to the original sequences (Table 1).

Following the suggestion of Deber and colleagues, the main change that we made was the addition of lysine residues to the N and C termini (*43*, *44*). This approach is now used frequently in studies of hydrophobic peptides and has been shown to facilitate the chemical synthesis and purification, increase solubility, and minimize aggregation, without significantly altering the properties of the peptides in detergent micelles or lipid vesicles (*45*−*50*). Despite its wide use, the possibility that the lysines affect helicity remains a valid concern. In our study, very small quantities of some of the peptides with fewer lysines could be purified. These peptides displayed the same helicity propensity as the variants with more lysines, supporting the idea that the added lysines do not affect the overall helicity of the A_2a TM peptides.

Two other kinds of amino acid changes were made in three of the peptides: (i) To enable us to monitor the binding of the peptides in the membrane-mimic environment, we substituted F for W in TM2 and Y for W in TM5. These changes did not alter the secondary structure of the peptides; peptides without these changes displayed equivalent CD spectra. (ii) To avoid formation of disulfide bonds, at two positions in TM6, alanine was substituted for cysteine. Sequence alignments of A_2a with other adenosine receptors and other superfamily A GPCRs indicate that the substituted residues are not conserved, except Cys254 in TM6. However, Cys254 is not involved in ligand binding of A_2a receptors.

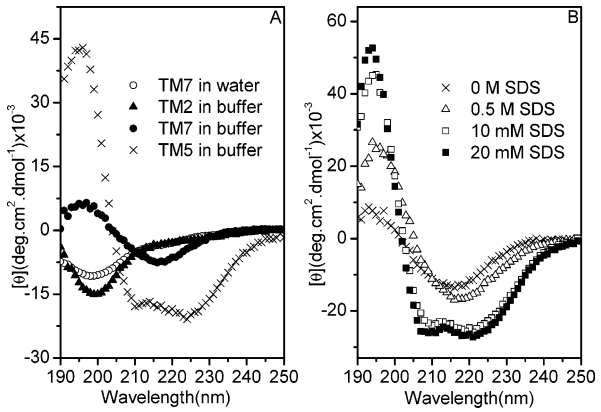

FIGURE 1: Representative CD spectra of TM peptides in water, buffer, and SDS micelles. (A) TM7 in H_2O (○); TM2 in 10 mM Tris buffer at pH 7.0 (▲); TM7 in 10 mM Tris buffer at pH 7.0 (●); and TM5 in 10 mM Tris buffer at pH 7.0 (×). (B) CD spectra of TM7 in increasing concentrations of SDS: 0 M SDS (×), 0.5 mM SDS (△), 10 mM SDS (□), and 20 mM SDS (■).

Prior studies have shown that the C254A mutation in A_2a does not alter ligand-binding properties, G protein coupling, or protein expression (*51*). The resulting peptide sequences were successfully synthesized and purified to >95% purity.

RESULTS

CD Spectra of Peptides in Water and Buffer. We sought to establish general features of the A_2a TM peptides, by collecting CD spectra of the peptides in aqueous and hydrophobic environments. First, far-UV CD spectra of peptides were recorded in two aqueous solutions: water and buffer. Figure 1A shows the CD spectra of representative peptides in water and in 10 mM Tris buffer at pH 7. In water, all seven TM peptides display the random-coil conformation, as seen by the single negative band in the 196−200 nm range (*52*). Although we do not have any evidence for aggregation of the peptides in water, we cannot rule out the possibility that monomers associate to some degree in water. However, the presence of the unordered structure suggests that the peptides are not aggregated probably because electrostatic repulsion by the positively charged Lys on both termini overcomes the tendency of hydrophobic peptides to self-associate. However, in Tris buffer, the peptides behave differently (Figure 1A). Three of the peptides, TM1, TM2, and TM4, remain in a random coil, similar to their conformation in water. The other four peptides apparently adopt relatively well-defined structures. The CD spectra of TM3, TM6, and TM7 show broad negative peaks at about 218 nm and positive peaks at about 198 nm, indicative of the β-strand structure. It is likely that these forms represent peptides that are associated to form β sheets. In aqueous buffer, unlike the rest of the peptides, TM5 adopts an α-helical structure with characteristic double minima at 222 and 207 nm and a positive maximum at 192 nm (Figure 1A). CD spectra of the peptides in the presence of salts such as KCI or NaCl were similar to those observed in Tris buffer (not shown).

To determine whether micelles could stabilize the folding of the peptides by providing hydrophobic environments, far-UV CD spectra of the TM peptides were recorded in the presence of increasing concentrations of SDS. The anionic SDS detergent was chosen because of the small size of the micelles that it forms and correspondingly low amounts of turbidity and light scattering (*53*, *54*). Figure 1B shows the CD spectra of TM7 recorded in the presence of different concentrations of SDS. At lower concentrations of SDS, well below the cmc (about 8.4 mM under our conditions), the peptide adopts a β-sheetlike structure, seen from the broad single negative minimum at about 218 nm. However, at SDS concentrations higher than the cmc, the peptide adopts a helical conformation, evident from the appearance of the double minima at 220 and 207 nm. The maximum effect of SDS on α helicity was measured at a concentration of the detergent of about 10 mM, which correlates with the micelle formation by SDS. Above this concentration, the features of the CD spectrum do not change. These data show that, despite forming β sheets in buffer, the peptide spontaneously forms an α-helical structure in the presence of SDS micelles.

Table 2: Fluorescence Emission Maxima and Stern−Volmer Constants (K_{SV}) of the TM Peptides in H_2O, Aqueous Buffer, and SDS Micelles

	H_2O	10 mM Tris at pH 7		SDS micelles	
peptide	λ_{max}	λ_{max}	K_{SV} (M^{-1})	λ_{max}	K_{SV} (M^{-1})
TM1	350	342	17.3	328	7.5
TM2	350	348	36.8	338	12.6
TM4	350	349	15.9	336	7.2
TM5	346	333	15.2	329	4.6
TM6	349	336	10	326	5.4
TM7	348	341	22	324	4.9

TM Peptide Insertion into Micelles. Prior to evaluating the secondary structure content of the peptides in micelles, we used fluorescence spectroscopy to confirm that the peptides insert into micelles in accordance with our design. The sensitivity of Trp fluorescence emission to the polarity of the environment allows us to use the Trp residues as reporter groups to monitor the binding of peptides to the micelles (*55*). Table 2 summarizes the data for the Trp fluorescence emission maximum (λ_{max}) and Stern−Volmer quenching constant (K_{SV}) measured in different media for the six peptides that contain Trp in their sequences (Table 1). In water, the Trp fluorescence emission maxima of the peptides are centered at around 348−350 nm (Figure 2A and Table 2). These values are typical for Trp residues in polar environments and for free Trp in water (*55*). In aqueous buffer, λ_{max} of TM1, TM2, and TM4 peptides show values close to those seen in water, while the Trp fluorescence emission maxima of TM5, TM6, and TM7 peptides are blue-shifted (at about 13 nm), suggesting partially buried Trp residues because of aggregation or self-association of the peptides (Table 2) (*35*, *56*). These findings agree with the secondary structures of the peptides revealed by CD.

Addition of the peptides to SDS micelles results in increases of the fluorescence intensity and significant blue shifts of λ_{max} by ~24 nm (parts A and B of Figure 2 and Table 2). These values are typical for buried Trp residues in hydrophobic environments and strongly suggest that the peptides insert into micelles (*55*). The insertion of the peptides into micelles was further supported by fluorescence-quenching measurements using the neutral water-soluble quencher acrylamide. Parts C and D of Figure 2 show representative Stern−Volmer plots for the quenching of Trp fluorescence in TM4 and TM7 peptides by acrylamide, recorded in the absence and presence of SDS micelles.

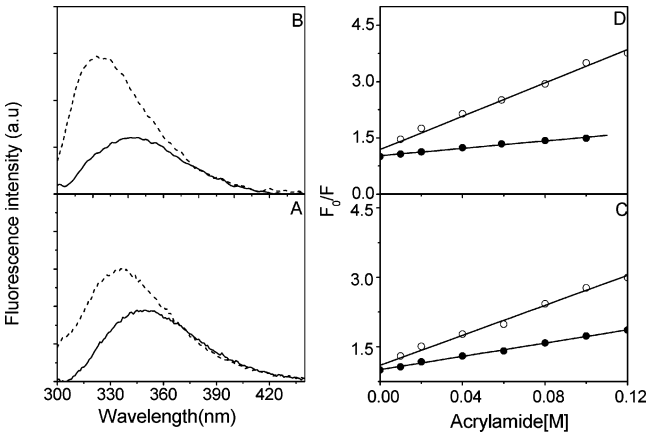

FIGURE 2: Representative fluorescence spectra and Stern−Volmer plots of TM peptides. Left panel: (A) Fluorescence emission spectra of TM4 in the presence of water (—) and SDS micelles (- - -). (B) Fluorescence emission spectra of TM7 in 10 mM Tris buffer at pH 7.0 (—) and SDS micelles (- - -). Right panel: Stern−Volmer plots for acrylamide quenching of Trp fluorescence for the TM4 peptide (C) and the TM7 peptide (D) in the presence of 10 mM Tris buffer at pH 7.0 (○) and SDS micelles (●). Fluorescence spectra were recorded at 25 °C, with excitation at 295 nm; fluorescence intensity was measured in the absence (F_0) and in the presence (F) of acrylamide.

Increasing the concentration of quencher to the peptide solutions resulted in decreases in the fluorescence intensity in both media; however, this effect is stronger in the presence of micelles than in the buffer alone. Thus, the values for the Stern−Volmer quenching constants for both peptides are reduced by about 2−4-fold in the presence of SDS micelles, indicating that Trp residues are less accessible to the quencher and strongly suggesting that they are buried inside the micelles. Similar quenching profiles were measured for all peptides, except for TM2, which displayed highly efficient quenching in both in the presence and absence of micelles (Table 2).

Interestingly, the Stern−Volmer quenching constant (K_{SV}) of the TM2 peptide in the presence of SDS micelles is actually lower than it is in the buffer, although the magnitude of both K_{SV} values for TM2 are higher than those for the rest of the peptides. The TM2 peptide also undergoes a very small blue shift of λ_{max} in SDS micelles, suggesting that this peptide associates poorly with micelles. It is also possible that two different populations of TM2 exist, one unordered and the other α helical.

Altogether, the fluorescence data indicate that the TM peptides insert into SDS micelles. However, a comparison of Trp emission maximum and calculated Stern−Volmer quenching constants, K_{SV} values, illustrate some distinctive differences between peptides. In SDS micelles, λ_{max} of TM1, TM5, TM6, and TM7 peptides undergo the most significant blue shifts, which correlate with lower values for K_{SV}, whereas the λ_{max} of the TM4 peptide undergoes a small blue shift and the peptide has a relatively high K_{SV} in SDS.

Secondary Structure Content of TM Peptides in Micelles. In SDS micelles, all seven TM peptides form α-helical structures, as indicated by their far-UV CD spectra with double minima at 222 and 208 nm and a positive peak at about 192 nm (Figure 3). Despite their overall similarities, some differences among the peptides can be easily noted. In SDS micelles at 25 °C, four of the peptides (TM4, TM3, TM5, and TM7) exhibit very high helicity, over 80% for TM4 and >70% for TM3, TM5, and TM7. TM1 exhibits relatively high helicity (nearly 60%), whereas two of peptides TM6 and TM2 show low helicity, only 30 and 18%, respectively (Figure 6). In accordance with the fluorescence data showing its low tendency to insert into SDS micelles, the TM2 peptide exhibits the lowest helicity among the seven peptides.

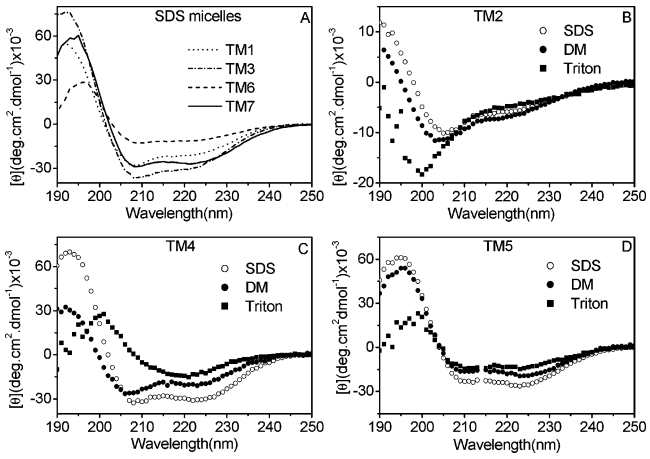

FIGURE 3: Representative CD spectra of TM peptides in detergent micelles. (A) UV CD spectra of TM1 (⋯), TM3 (-•-), TM6 (- - -), and TM7 (—) in the presence of SDS micelles. A comparison of CD spectra of TM2 (B), TM4 (C), and TM5 (D) peptides in the presence of SDS (○), Dβ M (●), and Triton X-100 micelles (■).

According to the predicted identity of the TMDs in the A_2a receptor (http://www.gpcr.org/7tm/), in each of our TM peptides, the TMDs comprise at about 72% of the amino sequence (i.e., excluding the additional lysine residues and the amino acids predicted to be in the intra- or extracellular loops). From CD analysis, the TM portions of TM3, TM4, TM5, and TM7 peptides display 100% helicity in the presence of SDS micelles.

Several lines of evidence suggest that all of the peptides except TM5 are monomeric. For every peptide, except the TM5 peptide, the ratio of $[\theta]_{222}/[\theta]_{208}$ is less than 1. This ratio has been shown to be a marker characteristic of α-helical, monomeric peptides (*57*−*59*). The CD spectra of all peptides except TM5 were independent of the peptide concentration (not shown), further supporting the idea that these six peptides are inserted as monomers into the micelles and that they are single-stranded α helices. All peptides except TM5 appeared as single bands on SDS−PAGE with apparent MW ≈ 4000 Da, supporting the idea that the peptides are monomeric (not shown). In contrast, in both the buffer and micelles, the CD spectra of the TM5 peptide shows a $[\theta]_{222}/[\theta]_{208}$ ratio greater than 1, indicative of a coil-coiled structure (Figure 3D) (*57*). The TM5 peptide also displayed concentration dependence, suggesting that it forms oligomeric structures in aqueous and hydrophobic environments.

Helical propensities of the peptides were also tested in nonionic detergents: Dβ M and Triton X-100. Figure 3 shows representative CD spectra of the peptides in the presence of micelles from these three different detergents. In the presence of micelles formed by Dβ M, which carries the same 12 carbon hydrophobic tail as SDS, most of the peptides (TM1, TM3, TM5, and TM7) adopt α-helical structures, although

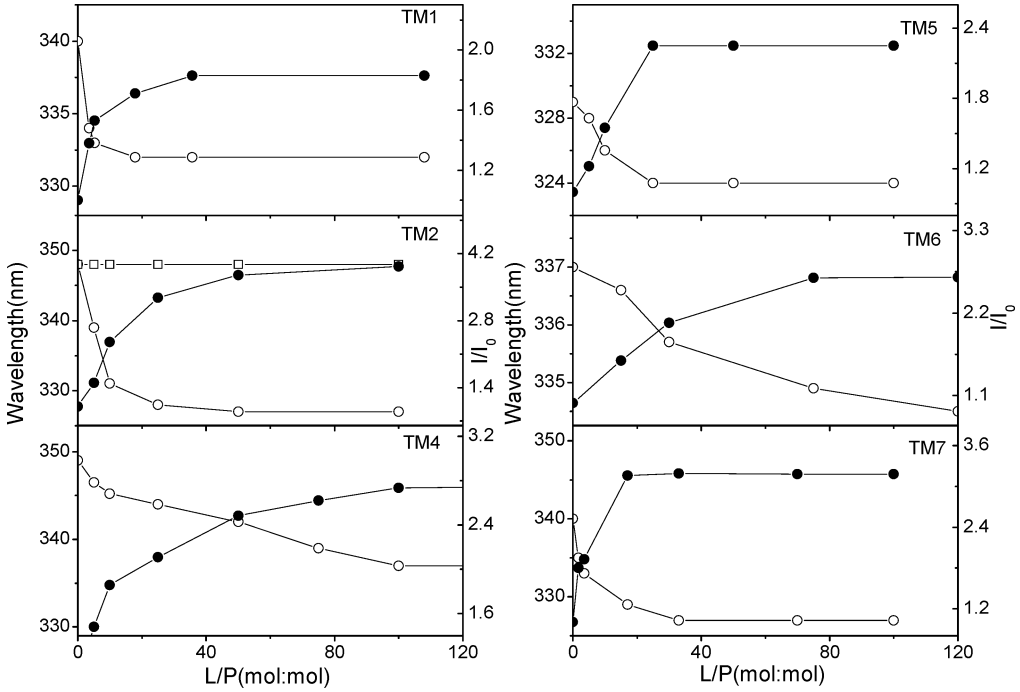

FIGURE 4: Interaction of TM peptides with DMPC vesicles. Fluorescence maximum (○) and fluorescence intensity (●) as a function of L/P molar ratio for TM1, TM2, TM4, TM5, TM6, and TM7. For the TM2 peptide, the data presented are for DMPC/DMPG vesicles and for DMPC (□).

in all cases, their apparent helicity is reduced relative to that observed in SDS micelles. These results indicate that the hydrophobic potential of the detergent alone is not enough to stabilize the helical structure and that electrostatic interactions can be important for insertion and initiation of the folding process.

In the Triton X-100 micelles, the peptides form different secondary structures. None of the peptides except TM5 forms α-helical conformation. TM2 fails to adopt any ordered structure. For the rest of the peptides in Triton X-100, the β-sheetlike structure appears to be a preferred conformation, as judged from the broadness of the CD spectra between 208 and 220 nm.

Insertion of TM Peptides into Lipid Vesicles. Because lipid vesicles simulate membrane structures more accurately than detergent micelles, we sought to characterize the properties of the A_2a TM peptides in vesicles. Before evaluating the secondary structures of the peptides, we tested their ability to insert into model membranes formed from DMPC (or DMPC/DMPG) vesicles. Trp emission maximum (λ_{max}) and fluorescence intensity were used to demonstrate the interaction of the peptides with lipid vesicles (*60*). Lipid titrations were performed by adding small aliquots of concentrated lipid vesicle suspensions (zwitterionic DMPC and negatively charged DMPC/DMPG vesicles) to the peptide at a constant concentration (~2 μM), following the procedure described in the Materials and Methods. Figure 4 shows the dependence of λ_{max} and fluorescence intensity on lipid/protein (L/P) molar ratio.

For all peptides, except TM2, addition of DMPC vesicles results in a blue shift in λ_{max} and an increase in fluorescence intensity of about 3−4-fold. These changes are expected when Trp residues move from a polar to a more nonpolar environment, suggesting penetration of the peptides into the hydrophobic part of the bilayer. Note that no binding to DMPC vesicles was observed for the TM2 peptide, because λ_{max} and fluorescence intensity were both invariant over the entire range of the L/P molar ratio (Figure 4B). Addition of the TM2 peptide to negatively charged DMPC/DMPG vesicles, however, caused a progressive blue shift of λ_{max} and an increase in fluorescence intensity.

The changes of fluorescence spectral characteristics strongly imply an insertion of the peptides into the lipid bilayer. The different L/P ratios at which the binding curves reach saturation suggest that different peptides have different affinities for binding to (or inserting into) the lipid bilayers. For TM1, TM5, and TM7 peptides, binding saturates at the lowest L/P ratio, indicating higher affinity to DMPC. TM4 binds with modest affinity. TM6 has low affinity, and TM2 has no measurable affinity for DMPC vesicles. Affinity of TM2 for mixed DMPC/DMPG vesicles was modest (similar to that of TM4 for DMPC).

Secondary Structure Content of TM Peptides in Vesicles. CD spectra of all TM peptides in the presence of vesicles have two minima at 222 and 208 nm and a positive maximum at 192 nm, indicating a helical conformation (Figure 5). On the basis of the CD spectra, six of the seven TM peptides are helical in both DMPC and DMPC/DMPG (not shown) vesicles; the TM2 peptide only appears to adopt a helical conformation in DMPC/DMPG (Figure 5B). The apparent random-coil structure of the TM2 peptide in the presence of DMPC is consistent with its failure to associate with these vesicles, as revealed by fluorescence. Even at the highest L/P molar ratio, the CD spectrum of the TM2 peptide was essentially the same as in the buffer alone. However, in mixed DMPC/DMPG vesicles, where binding was observed by fluorescence, the peptide forms a stable α-helical structure, although with relatively low helicity (Figure 5B and Figure 6). As observed in SDS micelles, the CD spectra of all peptides, except the TM5 peptide, show a $[\theta]_{222}/[\theta]_{208}$

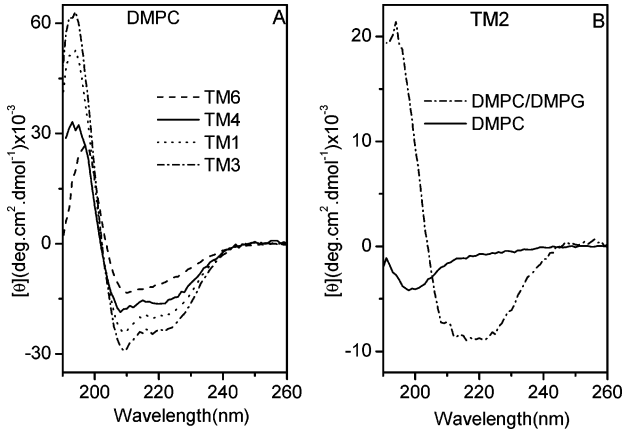

FIGURE 5: Representative CD spectra of TM peptides in lipid vesicles. (A) UV CD spectra of TM1 (•••), TM3 (-•-), TM6 (- - -), and TM4 (—) peptides in the presence of DMPC vesicles at 25 °C. (B) CD spectra of TM2 in the presence of DMPC (—) and DMPC/DMPG (-•-) vesicles.

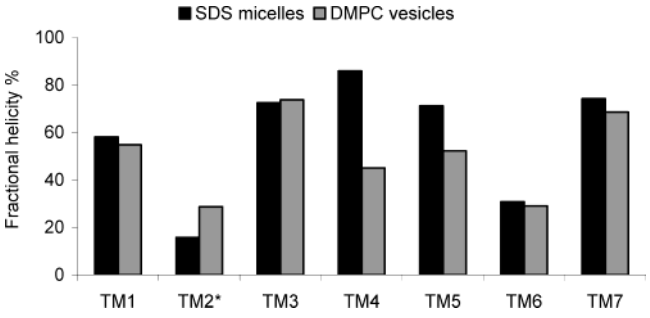

FIGURE 6: Fractional helicity for the seven peptides in the presence of SDS micelles and DMPC vesicles. The asterisk indicates that the data presented for TM2 are in DMPC/DMPG vesicles. All measurements were performed at 25 °C.

ratio of less than 1, indicative of the monomeric helical structure of the peptides in lipid bilayers.

For TM1, TM3, TM6, and TM7 peptides, the percent helix content in DMPC vesicles at room temperature are similar to the values in SDS micelles. For TM4 and TM5 peptides, helicity in DMPC was somewhat lower than in SDS. The TM2 peptide was more helical in DMPC/DMPG than in SDS micelles (Figure 6). As with SDS micelles, substantial differences in the helical content were observed for the different TM peptides. The rank order of helicity in DMPC vesicles was TM3 > TM7 > TM5 ≈ TM1 > TM4 > TM2 ≈ TM6. This order differs somewhat from the rank order of the helicity of the peptides in SDS (TM4 > TM7 ≈ TM5 ≈ TM3 > TM1 > TM6 > TM2).

Thermal Stability of TM Peptides in Membrane-Mimetic Environments. The thermal stability of the peptides inserted in SDS micelles and vesicles was studied by collecting CD spectra of all seven peptides at temperatures up to 95 °C in the presence of SDS micelles and DMPC vesicles (not shown). Similar trends were recorded for all TM peptides. Heating to 45 °C causes very small changes in the helicity of the peptides. A further increase of temperatures up to 95 °C induces a more significant decrease of α helicity; however, the peptides are still folded and highly helical. Cooling the samples back to 25 °C results in recovery of the initial spectra, indicating reversibility of the process.

TM peptides are relatively more stable in vesicles than in SDS micelles. An increase of temperatures up to 95 °C results in a loss of only ∼15% in helicity, while in SDS micelles, heating to 95 °C causes a loss of ∼25% for most of the peptides (not shown).

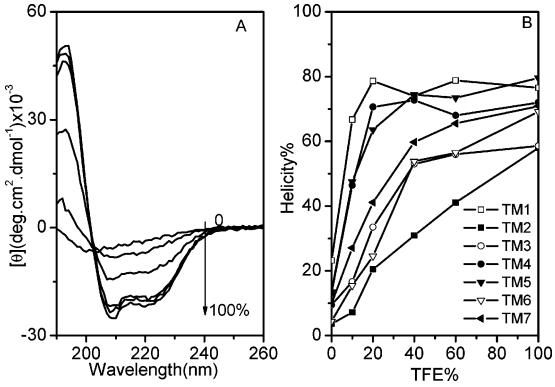

FIGURE 7: Effects of TFE on the TM peptide secondary structure. (A) CD spectra of the TM7 peptide as a function of the TFE concentration. The spectra are recorded in the absence of TFE (water) and in TFE/water mixtures with the increasing percentages of TFE: 10, 20, 40, 60, and 100%. (B) Calculated values for helicity of the seven peptides TM1 (□), TM2 (■), TM3 (○), TM4 (●), TM5 (▼), TM6 (▽), and TM7 (tilted ▲) as a function of the TFE concentration.

Secondary Structure of TM Peptides in TFE/H_2O Mixtures. The A_2a peptides exhibit markedly different helical propensities in micelles and vesicles. To test whether these differences are affected by poor solubility of the peptides in these environments, we examined the helical propensity of the peptides in the presence of TFE, known to induce the helical structure. In TFE/H_2O mixtures, all peptides form helical structures, with the amount of helicity increasing with an increasing concentration of TFE up to a maximal plateau value (Figure 7).

The CD spectra of all peptides except TM6 exhibit an isobestic point at 202 nm, indicative of a two-stage equilibrium between random-coiled and helical conformations (representative spectra shown in Figure 7A). For five of the seven peptides (TM2 and TM6 are the exceptions), the induction of the helix occurs mostly in the range of 0 to 40% TFE/H_2O. Above this concentration, little change is observed and the helical percentage plateaus (Figure 7B). Dependence of helicity on the TFE concentration is believed to be an intrinsic property of peptides (*20*). In agreement with the data from the membrane-mimic experiments among the seven peptides, TM2 and TM6 peptides display the lowest helical propensities at almost all TFE/H_2O ratios. Thus, we believe all of the peptides are able to form a helical structure, and the observed differences in their helicity reflect genuine conformational preferences.

DISCUSSION

The aim of our study was to improve the understanding of the forces and mechanisms governing GPCR-folding and -assembly processes. We have designed peptides corresponding to the seven TM domains of the human adenosine A_2a receptor and characterized their helical propensity in membrane-mimetic environments and their tendency to associate with micelles and lipid vesicles. Because of the high hydrophobicity of putative TMDs, we flanked each TM domain with several Lys residues on both termini to increase

their solubility. Thus, all seven designed peptides share similar chain lengths of about 30−33 amino acid residues, with 23−25 residues representing the putative TMDs.

CD spectra of the peptides in water indicate that the peptides have a random-coil structure, indicating that repulsive electrostatic interactions prevent the formation of aggregates typical for hydrophobic peptides. However, in aqueous buffers (or in the presence of salt), three of the peptides (TM3, TM6, and TM7) adopt a β-sheetlike structure, while the TM5 peptide folds into a helical structure. The formation of these structures in aqueous buffer is probably initiated by neutralization of the positive charges of Lys residues by buffer anions (or salt), which in turn leads to aggregation or self-association driven by hydrophobic interactions. Despite this tendency to form β sheets in buffer, when the peptides encounter micelles and vesicles, all seven readily form independent helices. These results emphasize that hydrophobic interactions are a major determinant for the folding of TMDs.

Although all of the seven TM peptides form some degree of independent helical structures in membrane-mimetic environments, they display significant variability in their helical propensity and tendency to insert into or associate with micelles and vesicles. Overall, peptides TM3, TM4, TM5, and TM7 are the most helical, and TM1 is intermediate, while TM6 and TM2 are the least helical. All seven peptides efficiently formed helices in TFE/water mixtures, confirming that they are competent to form the helical structure, and the differences in helicity that we observe in micelles and vesicles reflect genuine differences in their intrinsic helical propensity and stability.

Moreover and most revealingly, none of these properties correlates well with overall hydrophobicity (Table 1). The calculated average hydrophobicity of the seven TM peptides is in the range of 1.5−2.39 based on the Kyte−Doolittle scale (*61*). Prior studies with model peptides have shown that the relative helicity of polypeptide segments in lipid systems correlates with their average segmental hydrophobicity (*62*). However, with the peptides from the A_2a receptor, we did not find a correlation between hydrophobicity and helical propensity of the peptides. TM2 and TM6 are among the most hydrophobic, yet they are the least helical. TM2 incorporates least efficiently into micelles and vesicles. In contrast, TM4 and TM7 peptides are the least hydrophobic, yet they are among the most helical in both micelles and vesicles. Thus, for example, the low helicity of TM2 and TM6 peptides must be attributed to effects derived from specific amino acid sequence effects, rather than to the hydrophobic effect.

Inspection of the sequences of these peptides does not reveal any obvious explanation for the differences in their helicity. Helical content does not correlate with overall hydrophobicity, nor does the presence of proline residues correlate with lower helicity. The last finding is consistent with recent analyses of studies that indicate that proline, known as a helix breaker in aqueous solutions, shows greatly enchanted helical propensity in the membrane-mimic environment and organic solvents (*63*). We believe that helix formation and membrane insertion of TMDs are likely to be complex processes, mediated by a variety of forces, including intrahelix interaction, which may occur before or after insertion into the membrane.

Helix formation by these peptides in micelles strongly depends on the nature of the detergents. Micelles of the neutral detergent DβM induced much less helical structure than did micelles formed from the anionic detergent SDS. The two detergents have similar hydrophobic potential and carry the same C_{12} hydrophobic tail. These results indicate that the hydrophobic potential of the detergent alone is not enough to stabilize the helical structure and electrostatic interactions that can play a significant role in the insertion of TMDs and the initiation of the helix formation and folding. Electrostatic interactions between peptides and negatively charged lipids have been proposed as driving forces for binding of peptides to membranes (*14*, *64*).The magnitudes of the electrostatic effects vary among the A_2a TM peptides, in that the conformation of some peptides are much more sensitive to the detergent charge than others. Because all A_2a TM peptides have a similar number of positive-charged Lys on their ends, we believe that the different electrostatic effects result from sequence variation in the TMDs.

In the presence of Triton X-100 micelles, the TM peptides display significant structural diversity. In this environment, of the seven peptides, only the TM5 peptide forms a helical structure; the rest form mostly β sheets. This behavior probably results from hydrophobic mismatch of the TM regions of the peptides with the hydrophobic tail of the detergent. The nonionic detergent Triton X-100 has a shorter hydrophobic tail than DβM; it is likely that the mismatch disrupts the insertion process and makes helix formation in the peptides unfavorable.

Among the seven A_2a TM peptides, only the TM5 peptide displays a ratio of $[\theta]_{222}/[\theta]_{208}$ greater than 1, attributed to the presence of the coiled-coil structure (*65*). The presence of higher order oligomeric states of the TM5 peptide is intriguing and suggests a possible role for interactions between TM5 domains in theoligomerization of the A_2a receptor. Dimerization has been convincingly demonstrated using biophysical methods for several GPCRs, including A_2a (*66*, *67*). Recently, atomic force microscopy (AFM) images provided evidence for dimerization of rhodopsin molecules in rod outer segments of photoreceptor cells (*68*). GPCR dimerization has also been shown to play a role in mediating signaling, but the mechanisms of dimer formation have not been identified (*69*). The formation of stable coiled-coil structures by TM5 of A_2a suggests a mechanism for intermolecular association in A_2a receptors.

It is interesting to compare our findings with those from similar studies of other helical-membrane proteins. In the Ste2 receptor and in BR, TM6 peptides were the least helical, and it was suggested that this property relates to their putative role in signaling (*13*, *70*), because TM6 is involved in ligand binding and signal transduction in many GPCRs (*1*, *71*). Intriguingly, TM6 of A_2a is also among the least helical and displays conformational variability. These findings are consistent with a model in which flexibility needed for conformational changes during signaling is achieved at the expense of intrinsic helical stability. The lower helicity found in the TM6 peptide upon binding to membranes might be accounted for by its need to interact with the other helices. TM3 is also believed to undergo significant conformational changes upon GPCR activation. The finding that TM3 from Ste2 was a poor helix seemed to confirm the correlation suggested by the properties of TM6 (*11*). However, in A_2a,

TM3 is among the most helical, while TM2 is a poor helix. Thus, these properties differ among the GPCR family, either indicating that the relationships between helicity, conformational stability, and signaling mechanism are not conserved or that different TM helices can play different roles in GPCRs (*72*).

It is also interesting to interpret our findings in the context of membrane-protein folding. While it is tempting to think of helical-membrane proteins as modular and folding via a pathway reminiscent of the early framework models, evidence is accumulating that, in membrane proteins such as GPCRs and other seven-helix TM proteins, regions of the protein may be unstructured outside the context of the native structure (*73*). In A_2a, it is likely that at least TM2 and TM6 domains need interaction with other helices or with a preformed core to facilitate stabilization of their helical structures. However, the fact that A_2a TM2 has a low intrinsic helical propensity, while in BR, it can serve as a template for folding of the other TMDs, suggests that the folding pathways of membrane proteins will differ, even within the same structural motif.

Finally, the tendency of many of the A_2a TM peptides to associate and aggregate in aqueous or buffer environments suggests that, as for soluble proteins, formation of the native structure in membrane proteins also requires avoiding improper inter- and intrachain interactions that lead to aggregation.

Our studies lay the groundwork for more detailed analysis of the folding pathways for human GPCRs. Our findings suggest a model for A_2a-receptor folding that includes formation of a core helical domain, with additional helix formation upon assembly. The extent of helix−helix interactions, whether the TMDs interact prior to insertion, and the degree to which interhelix interaction drive helix formation are the subject of our current investigations.

ACKNOWLEDGMENT

We are grateful to Dr. Yu Sung Wu, Damien Thévenin, Matthew Roberts, and Pumtiwitt Rancy for many helpful discussions and assistance.

REFERENCES

1. Gether, U. (2000) Uncovering molecular mechanisms involved in activation of G protein-coupled receptors, *Endocr. Rev. 21*, 90−113.
2. Gurrath, M. (2001) Peptide-binding G protein-coupled receptors: New opportunities for drug design, *Curr. Med. Chem. 8*, 1605−1648.
3. Shichida, Y., and Imai, H. (1998) Visual pigment: G-protein-coupled receptor for light signals, *Cell Mol. Life Sci. 54*, 1299−1315.
4. Hakak, Y., Shrestha, D., Goegel, M. C., Behan, D. P., and Chalmers, D. T. (2003) Global analysis of G-protein-coupled receptor signaling in human tissues, *FEBS Lett. 550*, 11−17.
5. Grisshammer, R., and Tate, C. G. (1995) Overexpression of integral membrane proteins for structural studies, *Q. Rev. Biophys. 28*, 315−422.
6. Palczewski, K., Kumasaka, T., Hori, T., Behnke, C. A., Motoshima, H., Fox, B. A., Trong, I. L., Teller, D. C., Okada, T., Stenkamp, R. E., Yamamoto, M., and Miyano, M. (2000) Crystal structure of rhodopsin: A G protein-coupled receptor, *Science 289*, 739−745.
7. Karnik, S. S., Gogonea, C., Patil, S., Saad, Y., and Takezako, T. (2003) Activation of G-protein-coupled receptors: A common molecular mechanism, *Trends Endocrinol. Metab. 14*, 431−437.
8. Rashid, A. J., O'Dowd, B. F., and George, S. R. (2004) Minireview: Diversity and complexity of signaling through peptidergic G protein-coupled receptors, *Endocrinology 145*, 2645−2652.
9. Popot, J. L., and Engelman, D. M. (1990) Membrane protein folding and oligomerization: The two-stage model, *Biochemistry 29*, 4031−4037.
10. Hunt, J. F., Earnest, T. N., Bousché, O., Kalghatgi, K., Reilly, K., Horváth, C., Rothschild, K. J., and Engelman, D. M. (1997) A biophysical study of integral membrane protein folding, *Biochemistry 36*, 15156−15176.
11. Xie, H., Ding, F. X., Schreiber, D., Eng, G., Liu, S. F., Arshava, B., Arevalo, E., Becker, J. M., and Naider, F. (2000) Synthesis and biophysical analysis of transmembrane domains of a *Saccharomyces cerevisiae* G protein-coupled receptor, *Biochemistry 39*, 15462−15474.
12. Hunt, J. F., Rath, P., Rothschild, K. J., and Engelman, D. M. (1997) Spontaneous, pH-dependent membrane insertion of a transbilayer α-helix, *Biochemistry 36*, 15177−15192.
13. Popot, J. L., and Engelman, D. M. (2000) Helical membrane protein folding, stability, and evolution, *Annu. Rev. Biochem. 69*, 881−922.
14. Booth, P. J. (2003) The trials and tribulations of membrane protein folding in vitro, *Biochim. Biophys. Acta 1610*, 51−56.
15. Dawson, J. P., Melnyk, R. A., Deber, C. M., and Engelman, D. M. (2003) Sequence context strongly modulates association of polar residues in transmembrane helices, *J. Mol. Biol. 331*, 255−262.
16. DeGrado, W. F., Gratkowski, H., and Lear, J. D. (2003) How do helix−helix interactions help determine the folds of membrane proteins? Perspectives from the study of homo-oligomeric helical bundles, *Protein Sci. 12*, 647−665.
17. Peng, S., Liu, L. P., Emili, A. Q., and Deber, C. M. (1998) Cystic fibrosis transmembrane conductance regulator: Expression and helicity of a double membrane-spanning segment, *FEBS Lett. 431*, 29−33.
18. Booth, P. J. (1997) Folding α-helical membrane proteins: Kinetic studies on bacteriorhodopsin, *Fold Des. 2*, R85−R92.
19. Meijberg, W., and Booth, P. J. (2002) The activation energy for insertion of transmembrane α-helices is dependent on membrane composition, *J. Mol. Biol. 319*, 839−853.
20. Krishna, A. G., Menon, S. T., Terry, T. J., and Sakmar, T. P. (2002) Evidence that helix 8 of rhodopsin acts as a membrane-dependent conformational switch, *Biochemistry 41*, 8298−8309.
21. Muller, D. J., Kessler, M., Oesterhelt, F., Moller, C., Oesterhelt, D., and Gaub, H. (2002) Stability of bacteriorhodopsin α-helices and loops analyzed by single-molecule force spectroscopy, *Biophys. J. 83*, 3578−3588.
22. Johnson, A. E., and van Waes, M. A. (1999) The translocon: A dynamic gateway at the ER membrane, *Annu. Rev. Cell Dev. Biol. 15*, 799−842.
23. White, S. H., and Wimley, W. C. (1999) Membrane protein folding and stability: Physical principles, *Annu. Rev. Biophys. Biomol. Struct. 28*, 319−365.
24. Jayasinghe, S., Hristova, K., and White, S. H. (2001) Energetics, stability, and prediction of transmembrane helices, *J. Mol. Biol. 312*, 927−934.
25. Engelman, D. M., Chen, Y., Chin, C. N., Curran, A. R., Dixon, A. M., Dupuy, A. D., Lee, A. S., Lehnert, U., Matthews, E. E., Reshetnyak, Y. K., Senes, A., and Popot, J. L. (2003) Membrane protein folding: Beyond the two stage model, *FEBS Lett. 555*, 122−125.
26. Reddy, A. P., Tallon, M. A., Becker, J. M., and Naider, F. (1994) Biophysical studies on fragments of the α-factor receptor protein, *Biopolymers 34*, 679−689.
27. Wigley, W. C., Vijayakumar, S., Jones, J. D., Slaughter, C., and Thomas, P. J. (1998) Transmembrane domain of cystic fibrosis transmembrane conductance regulator: Design, characterization, and secondary structure of synthetic peptides m1−m6, *Biochemistry 37*, 844−853.
28. Deber, C. M., Liu, L. P., and Wang, C. (1999) Perspective: Peptides as mimics of transmembrane segments in proteins, *J. Pept. Res. 54*, 200−205.
29. Marti, T. (1998) Refolding of bacteriorhodopsin from expressed polypeptide fragments, *J. Biol. Chem. 273*, 9312−9322.
30. Yeagle, P. L., Choi, G., and Albert, A. D. (2001) Studies on the structure of the G-protein-coupled receptor rhodopsin including the putative G-protein binding site in unactivated and activated forms, *Biochemistry 40*, 11932−11937.

31. Fredholm, B. B., Cunha, R. A., and Svenningsson, P. (2003) Pharmacology of adenosine A_2A receptors and therapeutic applications, *Curr. Top. Med. Chem. 3*, 413−426.
32. Ribiero, J. A., Sebastião, A. M., and Mendoça, A. d. (2003) Adenosine receptors in the nervous system: Pathophysiological implications, *Prog. Neurobiol. 68*, 377−392.
33. Brandts, J. F., and Kaplan, L. J. (1973) Derivative sspectroscopy applied to tyrosyl chromophores. Studies on ribonuclease, lima bean inhibitors, insulin, and pancreatic trypsin inhibitor, *Biochemistry 12*, 2011−2024.
34. Henry, G. D., and Sykes, B. D. (1994) Methods to study membrane protein structure in solution, *Methods Enzymol. 239*, 515−535.
35. Ladokhin, A. S., Jayasinghe, S., and White, S. H. (2000) How to measure and analyze tryptophan fluorescence in membranes properly, and why bother? *Anal. Biochem. 285*, 235−245.
36. Eftink, M. R., and Ghiron, C. A. (1976) Exposure of tryptophanyl residues in proteins. Quantitative determination by fluorescence quenching studies, *Biochemistry 15*, 672−680.
37. Mao, D., and Wallace, B. A. (1984) Differential light scattering and absorption flattening optical effects are minimal in the circular dichroism spectra of small unilamellar vesicles, *Biochemistry 23*, 2667−2673.
38. Wallace, B. A., and Teeters, C. L. (1987) Differential absorption flattening optical effects are significant in the circular dichroism spectra of large membrane fragments, *Biochemistry 26*, 65−70.
39. Glaeser, R. M., and Jap, B. K. (1985) Absorption flattening in the circular dichroism spectra of small membrane fragments *Biochemistry 24*, 6398−6401.
40. Chen, Y. H., Yang, J. T., and Chau, K. H. (1974) Determination of the helix and β form of proteins in aqueous solution by circular dichroism, *Biochemistry 13*, 3350−3359.
41. Chang, C. T., Wu, C. S., and Yang, J. T. (1978) Circular dichroic analysis of protein conformation: Inclusion of the β-turns, *Anal. Biochem. 91*, 13−31.
42. Partridge, A. W., Melnyk, R. A., and Deber, C. M. (2002) Polar residues in membrane domains of proteins: Molecular basis for helix−helix association in a mutant CFTR transmembrane segment, *Biochemistry 41*, 3647−3653.
43. Melnyk, R. A., Partridge, A. W., and Deber, C. M. (2001) Retention of native-like oligomerization states in transmembrane segment peptides: Application to the *Escherichia coli* aspartate receptor, *Biochemistry 40*, 11106−11113.
44. Liu, L. P., and Deber, C. M. (1998) Guidelines for membrane protein engineering derived from de novo designed model peptides, *Biopolymers 47*, 41−62.
45. Bianchi, E., Ingenito, R., and Simon, R. A. (1999) Engineering and chemical synthesis of a transmembrane protein: The HCV protease cofactor protein NS4A, *J. Am. Chem. Soc. 121*, 7698−7699.
46. Wang, C., and Deber, C. M. (2000) Peptide mimics of the M13 coat protein transmembrane segment. Retention of helix−helix interaction motifs, *J. Biol. Chem. 275*, 16155−16159.
47. Zhou, F. X., Merianos, H. J., Brunger, A. T., and Engelman, D. M. (2001) Polar residues drive association of polyleucine transmembrane helices, *Proc. Natl. Acad. Sci. U.S.A. 98*, 2250−2255.
48. de Planque, M. R., Goormaghtigh, E., Greathouse, D. V., Koeppe, R. E., II, Kruijtzer, J. A., Liskamp, R. M., de Kruijff, B., and Killian, J. A. (2001) Sensitivity of single membrane-spanning α-helical peptides to hydrophobic mismatch with a lipid bilayer: Effects on backbone structure, orientation, and extent of membrane incorporation, *Biochemistry 40*, 5000−5010.
49. Ding, F. X., Xie, H., Arshava, B., Becker, J. M., and Naider, F. (2001) ATR−FTIR study of the structure and orientation of transmembrane domains of the *Saccharomyces cerevisiae* α-mating factor receptor in phospholipids, *Biochemistry 40*, 8945−8954.
50. Ding, F. X., Lee, B. K., Hauser, M., Patri, R., Arshava, B., Becker, J. M., and Naider, F. (2002) Study of the binding environment of α-factor in its G protein-coupled receptor using fluorescence spectroscopy, *J. Pept. Res. 60*, 65−74.
51. Kim, J., Wess, J., van Rhee, A. M., Schoneberg, T., and Jacobson, K. A. (1995) Site-directed mutagenesis identifies residues involved in ligand recognition in the human A2a adenosine receptor, *J. Biol. Chem. 270*, 13987−13997.
52. Sreerama, N., Venyaminov, S. Y., and Woody, R. W. (2001) Analysis of protein circular dichroism spectra based on the tertiary structure classification, *Anal. Biochem. 299*, 271−274.
53. Garavito, R. M., and Ferguson-Miller, S. (2001) Detergents as tools in membrane biochemistry, *J. Biol. Chem. 276*, 32403−32406.
54. Hoyt, D. W., and Gierasch, L. M. (1991) A peptide corresponding to an export-defective mutant OmpA signal sequence with asparagine in the hydrophobic core is unable to insert into model membranes, *J. Biol. Chem. 266*, 14406−14412.
55. Burstein, E. A., Vedenkina, N. S., and Ivkova, M. N. (1973) Fluorescence and the location of tryptophan residues in protein molecules, *Photochem. Photobiol. 18*, 263−279.
56. Lacowicz, J. (1999) *Principles of Fluorescence Spectroscopy*, 2nd ed., Kluwer Academic/Plenum Publishers, New York.
57. Zhou, N. E., Kay, C. M., and Hodges, R. S. (1992) Synthetic model proteins. Positional effects of interchain hydrophobic interactions on stability of two-stranded α-helical coiled-coils, *J. Biol. Chem. 267*, 2664−2670.
58. Lau, S. Y., Taneja, A. K., and Hodges, R. S. (1984) Synthesis of a model protein of defined secondary and quaternary structure. Effect of chain length on the stabilization and formation of two-stranded α-helical coiled-coils, *J. Biol. Chem. 259*, 13253−13261.
59. Melton, L. G., Church, F. C., and Erickson, B. W. (1995) Designed polyanionic coiled-coil proteins: Acceleration of heparin cofactor II inhibition of thrombin, *Int. J. Pept. Protein Res. 45*, 44−52.
60. Lew, S., Caputo, G. A., and London, E. (2003) The effect of interactions involving ionizable residues flanking membrane-inserted hydrophobic helices upon helix−helix interaction, *Biochemistry 42*, 10833−10842.
61. Kyte, J., and Doolittle, R. F. (1982) A simple method for displaying the hydropathic character of a protein, *J. Mol. Biol. 157*, 105−132.
62. Li, S. C., and Deber, C. M. (1993) Peptide environment specifies conformation. Helicity of hydrophobic segments compared in aqueous, organic, and membrane environments, *J. Biol. Chem. 268*, 22975−22978.
63. Li, S. C., Goto, N. K., Williams, K. A., and Deber, C. M. (1996) α-Helical, but not β-sheet, propensity of proline is determined by peptide environment, *Proc. Natl. Acad. Sci. U.S.A. 93*, 6676−6681.
64. Oren, Z., Ramesh, J., Avrahami, D., Suryaprakash, N., Shai, Y., and Jelinek, R. (2002) Structures and mode of membrane interaction of a short α helical lytic peptide and its diastereomer determined by NMR, FTIR, and fluorescence spectroscopy, *Eur. J. Biochem. 269*, 3869−3880.
65. Zhou, N. E., Kay, C. M., and Hodges, R. S. (1994) The role of interhelical ionic interactions in controlling protein folding and stability. De novo designed synthetic two-stranded α-helical coiled-coils, *J. Mol. Biol. 237*, 500−512.
66. Liang, Y., Fotiadis, D., Filipek, S., Saperstein, D. A., Palczewski, K., and Engel, A. (2003) Organization of the G protein-coupled receptors rhodopsin and opsin in native membranes, *J. Biol. Chem. 278*, 21655−21662.
67. Overton, M. C., and Blumer, K. J. (2000) G-protein-coupled receptors function as oligomers in vivo, *Curr. Biol. 10*, 341−344.
68. Fotiadis, D., Liang, Y., Filipek, S., Saperstein, D. A., Engel, A., and Palczewski, K. (2003) Atomic-force microscopy: Rhodopsin dimers in native disc membranes, *Nature 421*, 127−128.
69. Gouldson, P. R., Higgs, C., Smith, R. E., Dean, M. K., Gkoutos, G. V., and Reynolds, C. A. (2000) Dimerization and domain swapping in G-protein-coupled receptors: A computational study, *Neuropsychopharmacology 23*, S60−S77.
70. Lee, B. K., Lee, Y. H., Hauser, M., Son, C. D., Khare, S., Naider, F., and Becker, J. M. (2002) Tyr266 in the sixth transmembrane domain of the yeast α-factor receptor plays key roles in receptor activation and ligand specificity, *Biochemistry 41*, 13681−13689.
71. Huang, P., Li, J., Chen, C., Visiers, I., Weinstein, H., and Liu-Chen, L. Y. (2001) Functional role of a conserved motif in TM6 of the rat μ opioid receptor: Constitutively active and inactive receptors result from substitutions of Thr6.34(279) with Lys and Asp, *Biochemistry 40*, 13501−13509.
72. Yohannan, S., Faham, S., Yang, D., Whitelegge, J. P., and Bowie, J. U. (2004) The evolution of transmembrane helix kinks and the structural diversity of G protein-coupled receptors, *Proc. Natl. Acad. Sci. U.S.A. 101*, 959−963.
73. Luneberg, J., Widmann, M., Dathe, M., and Marti, T. (1998) Secondary structure of bacteriorhodopsin fragments. External sequence constraints specify the conformation of transmembrane helices, *J. Biol. Chem. 273*, 28822−28830.

BI0492051